https://doi.org/10.61092/iaea.wgk6-7vrs

INDC(NDS)-0868
Distr. G,NM,PH

IAEA
International Atomic Energy Agency

INDC International Nuclear Data Committee

Comparison of Photon Strength Functions from the OSLO Method with Neutron Capture Systematics

Jiri Kopecky
JUKO Research
Alkmaar, The Netherlands

František Bečvář
Charles University
Prague, Czech Republic

November 2022

IAEA Nuclear Data Section
Vienna International Centre, P.O. Box 100, 1400 Vienna, Austria

Selected INDC documents may be downloaded in electronic form
from *http://nds.iaea.org/publications*
or sent as an e-mail attachment.
Requests for hardcopy or e-mail transmittal should be directed to
NDS.Contact-Point@iaea.org
or to:
Nuclear Data Section
International Atomic Energy Agency
Vienna International Centre
PO Box 100
1400 Vienna
Austria

Printed by the IAEA in Austria

November 2022

INDC(NDS)-0868
Distr. G,NM,PH

Comparison of Photon Strength Functions from the OSLO Method with Neutron Capture Systematics

Jiri Kopecky
JUKO Research
Alkmaar, The Netherlands

František Bečvář
Charles University
Prague, Czech Republic

November 2022

Contents

1. INTRODUCTION 7
2. THE ORIGINAL ^{57}Fe RESULTS 7
3. ESSENTIALS OF ADOPTED OSLO METHOD DATA 9
   3.1. Absolute normalization and Eγ dependence 9
   3.2. Data uncertainties 13
4. CONCLUSIONS 15
   4.1. OSLO PSF shape and absolute normalization 15
   4.2. OSLO uncertainties 16
   4.3. Future possibilities 16
Acknowledgments 17
Technical remarks 17
References 17

1. INTRODUCTION

Since the mid-sixties, a wealth of data on photon strength functions (PSF) was obtained from neutron capture studies introduced by the Chalk River group [1]. The thermal and resonance capture measurements method was applied, and in the eighties, it was accompanied by a novel technique, the average resonance capture (ARC) method using filtered B, Sc, and Fe neutron beams [2]. This method increased the accuracy of the data by decreasing the Porter-Thomas fluctuations and allowed for the interpretation of the PSF within the Giant Dipole Resonance (GDR) model [3]. The energy range of primary transitions that was covered by these measurements was from about 4 MeV up to the neutron binding energy. This high energy region of PSF has been interpreted by many phenomenological models, from the standard Lorentzian SLO and many more variants, up to the recent SMLO [4]. The study of the low energy PSF component for E1 radiation was first proposed by Kadmenskij and Furman [5] and extended later by Kopecky and Uhl in Refs [6,7] (see the figures therein).

This novel treatment of the PSF shape was based on the introduction of the energy dependence of the GDR width $\Gamma_0(E_\gamma)$ and the nuclear temperature T of the final states, which influence the E1 properties. The $\Gamma_0(E_\gamma)$ energy dependence was verified by the observed PSF shape, but experimental confirmation of the nuclear temperature dependence was missing. The reason was that the primary neutron capture DRC and ARC transitions at low energies were difficult to observe and/or to assign, for reasons purely to do with experimental limitations. Direct access to low E_γ energies is possible in the thermal neutron capture measurements for light mass nuclei ($A < 60$) and the role of E1 direct capture is discussed in Refs [8,9]. When extending to heavier nuclei, using the shape trend analysis (see Refs [10,11]) and data with E_γ between 3 – 5 MeV, limits of the PSF of about $(1 \pm 0.5)\ 10^{-8}$ MeV^{-3} have been obtained with an exponential function extending to $E_\gamma \sim 0$. This estimate is in reasonable agreement with predictions from the GSLO model [6,7]. However, any theoretical support for M1 behavior was and is still missing.

Since the mid-nineties, numerous data on PSFs were obtained from studies of light-ion-induced photon production by means of a novel technique known as the Oslo method (OM), see, e.g. Ref. [12]. With this technique PSF data can be measured down to about $E_\gamma = 1$ MeV. A low-energy enhancement (LEE) effect, sometimes called the "upbend", of the dipole PSF below gamma-ray energies of 3 MeV, has been measured since 2004 for many nuclides with masses $44 < A < 250$. It was first reported for $^{56;57}$Fe nuclei [13] and further supported for several Mo isotopes [14]. These findings attracted wide attention, but it was hard to interpret this effect within the known modes of nuclear motion in existing theoretical models, partially due to the fact that the measured transitions corresponding to the dipole mode are identified without any spin/parity assignment.

2. THE ORIGINAL ^{57}Fe RESULTS

The size of the LEE component in the original OSLO ^{57}Fe experiment, chosen here for demonstration, is compared in Fig.1 with two recent theoretical photo-absorption models, the phenomenological SMLO model [4] and the microscopic D1M + QRPA model 15]. The detected gamma transitions which are analyzed without using any spin/parity information, result in the determination of the dipole (E1 + M1) mode, neglecting the quadrupole transitions. The strong enhancement of low energy PSF is shown in Fig.1 starting below 4 MeV.

The high energy absolute PSF data is validated by comparing with the <<f(E1)>> systematics derived from the average DRC data at <6.5 $\pm$ 0.5 MeV> and extended with the <4 MeV> point, derived from the D1M + QRPA energy E_γ (4/6.5) ratio calculation [10,16]. The M1/E1 ratio for high energy transitions in ^{57}Fe lies between 0.1 – 0.2 and thus the E1 systematics can safely be used for the absolute PSF normalization above 5 MeV and the <6.5> MeV value is completely independent of any model input.

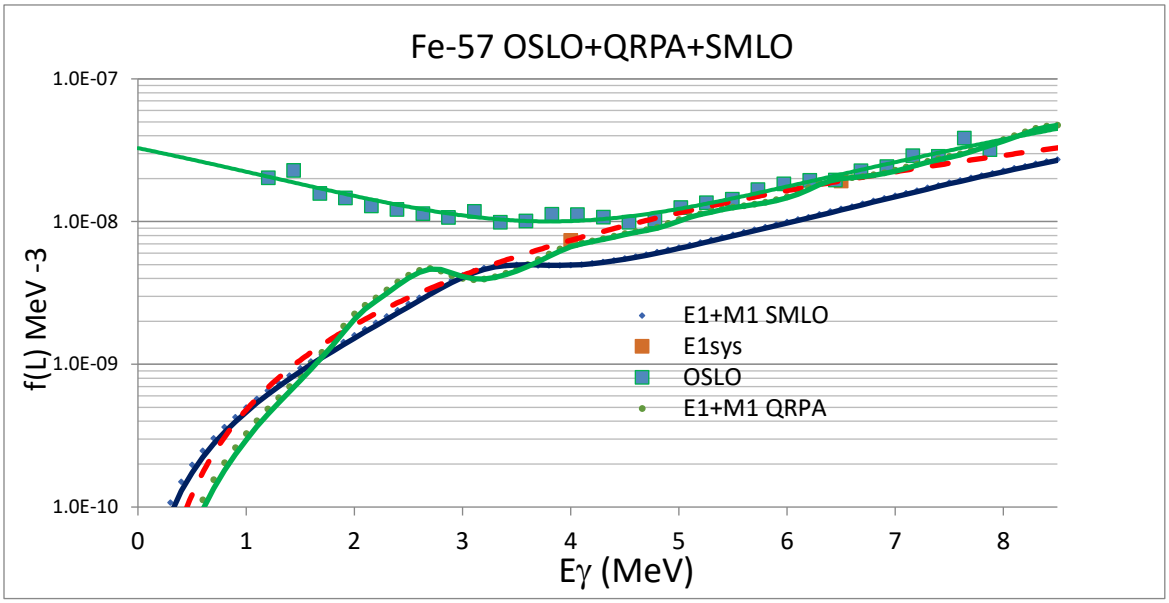

FIG.1. The OSLO data from the ^{57}Fe(^{3}He,^{3}He)^{57}Fe reaction. Note the increasing trend (dark green curve) towards the zero-energy limit starting at about 4 MeV. The quoted errors are remarkably small (~ 10%) and this fact will be discussed further. The D1M + QRPA (green dots and curve) and SMLO (blue dots and curve) calculations of the summed E1 and M1 PSF are included. Note the good agreement with the <<f(E1)>> systematics (red dashed curve) above 5 MeV also with the D1M + QRPQ values and the presence of the scissor resonance between 2 – 3 MeV, however, the latter is generally expected for deformed nuclei.

The theory has been extended by the postulation of a phenomenological "upbend lim0" term introduced separately for E1 and M1 modes, see Ref. [17]. Exponential functions decreasing with E_γ for E1 and M1 strength, adjusted to shell model calculations and OSLO results, were introduced, and implemented in both models (D1M + QRPA and SMLO) and the results are shown in Fig. 2 for the added E1 and M1 components. The size of the LEE component is visible in Fig. 1 and must contain the E1 and M1 strength responsible for the introduced "upbend". The trend analysis of the M1 thermal capture data indicates increasing strength towards low transition energies [10]. Results of the theoretical calculations, extended by the upbend lim0 component from Ref. [17], are shown for ^{57}Fe in Fig.2.

The best way to clarify this new LEE feature is to study its behavior globally across the entire mass region of available OSLO measurements. This approach may give better insight into the normalization of the phenomenological component of the theoretical models at low energies.

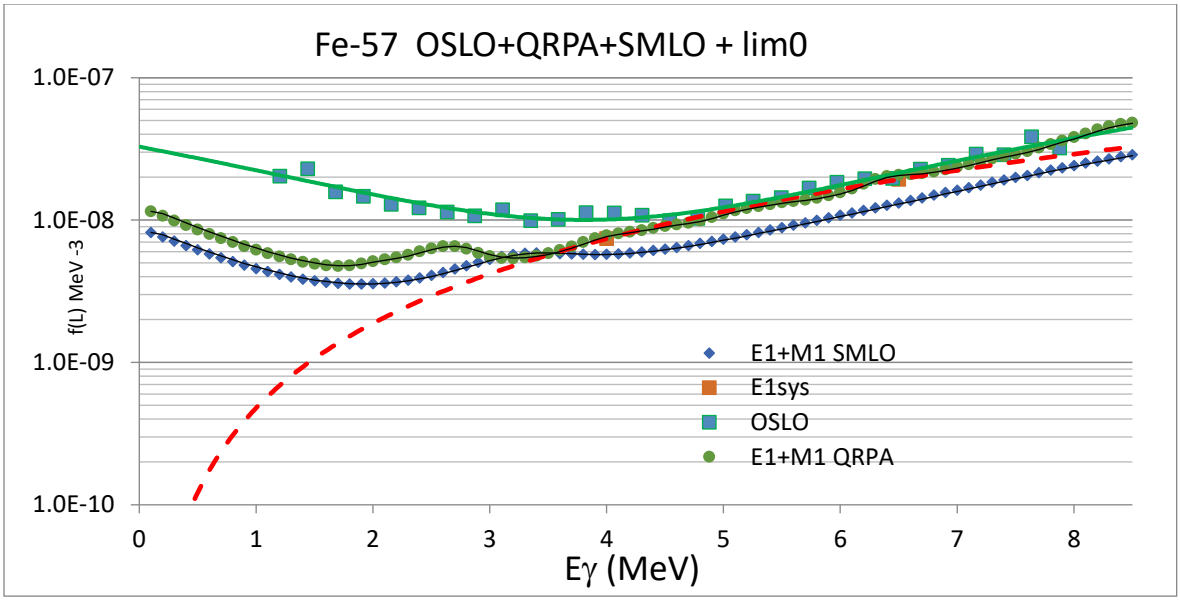

FIG. 2. The OSLO data from the $^{57}Fe(^{3}He,^{3}He)^{57}Fe$ reaction. The D1M + QRPA (green) and SMLO (blue) lim0 calculations of summed E1 and M1 PSF are plotted. The <<f(E1)>> systematics is the orange symbol and red dashed curve. Note that the proposed theoretical upbend components are about three to four times weaker at $E_\gamma \sim 0$.

3. ESSENTIALS OF ADOPTED OSLO METHOD DATA

The recent IAEA Coordinated Research Project (see: https://www.iaea.org/projects/crp/f41032) has produced a comprehensive compilation of experimental Photon Strength Functions [18] obtained using different experimental methods. The OSLO data collection includes 80 nuclides with masses 44 < A < 243 and forms, together with the neutron capture data, the two largest data sets with a common mass range. The importance of the neutron capture data lies in the absolute scaling of the PSF which has been successfully verified by theoretical predictions. It seems, therefore, that a comprehensive comparison with the OSLO data could be a valuable verification for the general PSF conclusions.

The basis of such a study was first to generate plots comparing all OSLO entries with data from other methods, if available. The '*OSLO+PSF plot.docx'* file includes graphical comparisons of OSLO data with other PSF data and the <<f(E1)>> systematics at <6.5> MeV (see Sec. 4.1). The complete plot file is available from the authors, however, its size prevents its inclusion in this paper. The OSLO data has been addressed from several perspectives as follows.

3.1. Absolute normalization and Eγ dependence

The OSLO method consists of several experimental and calculational steps, for a detailed description see Ref. [10] and refences therein. The method is based on the measurement of the particle-γ coincidence data which is sorted into a matrix of initial excitation energy E_i of the final nuclide versus the γ-ray deexcitation energy Eγ. For each of the excitation energy bins, the corresponding γ-ray spectra are unfolded, and the distribution of primary γ-rays is obtained for each excitation energy bin by means of an iterative technique. The nuclear level density $\rho(E_f)$ at the excitation energy $E_f = E_i - E_\gamma$ is used, with the normalization to experimental data (low energy discrete levels and D_o). The total γ-ray transmission coefficient, T_γ (E_γ) = T_{M1}+ T_{E1} (assuming

dominance of the dipole transitions), related to the primary γ-ray spectrum, is then determined and normalized to the average radiative width $<\Gamma_\gamma>$. In the readme files of the OSLO database this normalization is described as '*absolute value of the level density and transmission coefficient are found by normalization to known values*'. We assume that the OSLO data analysis carried out more than 20 years ago remains valid today.

The shape of a typical OSLO PSF f1(E_γ) function has three dominant energies, see Fig. 1. The data at the lowest measured E_γ (the LEE component), the middle energy at around 4 MeV (the M1 strength is comparable with the E1 mode) and the high energy region with $E\gamma > 5$ MeV, where the E1 is dominant, and the statistical E1 GDR model is widely applicable.

The high energy region (<6.5 MeV>) - The average PSF OSLO data is compared with the <<f(E1)>> systematics from the DRC experiment and with the D1M + QRPA calculations averaged over a (6.5 ± 0.5) MeV energy range with no upbend component. The model-free DRC data forms a clean experimental basis supported by the theory to determine the absolute PSF values. The overall average behaviour of the OSLO data for A > 150 data agrees reasonably with the expected energy dependence. For A < 150 the data is significantly dispersed and does not follow the expected GDR power shape. The stepwise change of the A < 150 and A > 150 data looks clear, especially if the small statistical uncertainties of the OSLO data are considered.

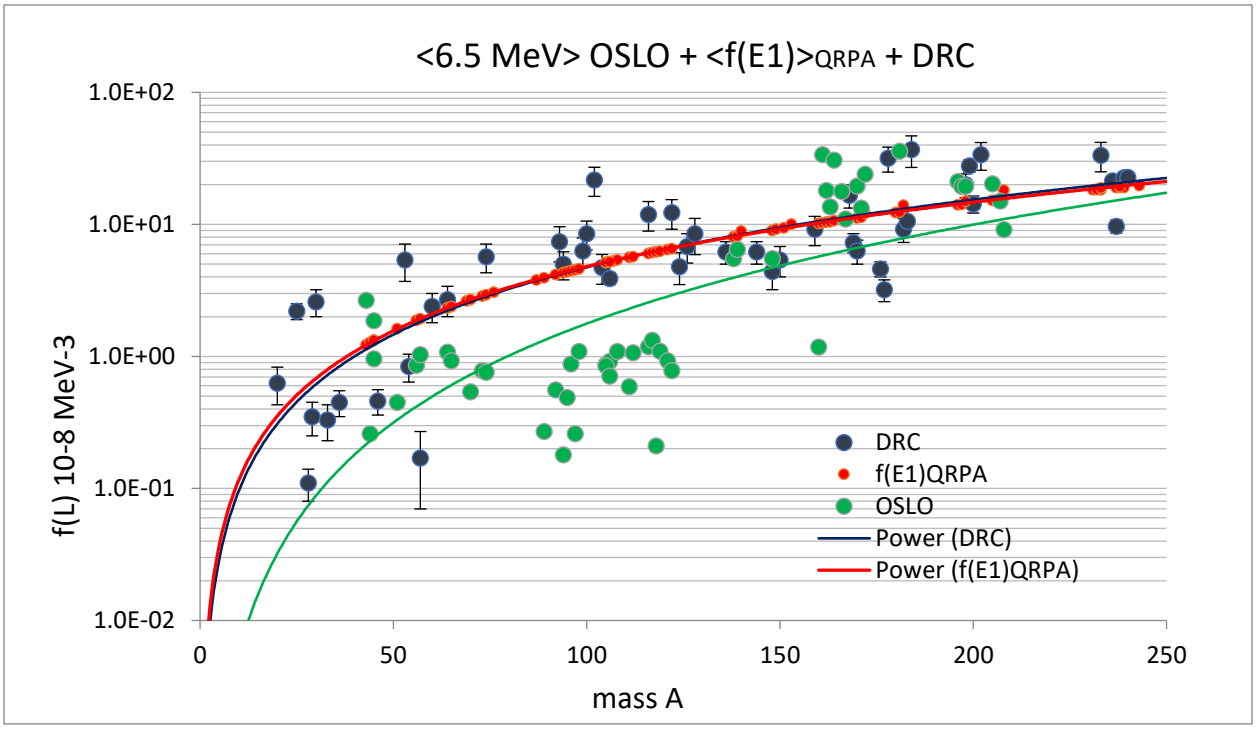

FIG.3. Comparison between the E1 experimental OSLO and the DRC data, with the <<f(E1)>> systematics curve, all data has been averaged within the (6.5±0.5) MeV bin. Note the remarkable agreement between the DRC and theoretical systematic predictions (the blue and red curves are almost identical). The power trend fit (green curve) is also applied for the OSLO data, but the data points show a sharp step dependence between data below and above A ~ 150.

The medium energy region (<4.0 MeV>) – The medium point at <4 MeV> is shown in Fig. 4 and gives slightly different results. The data dispersion is smaller, which may indicate smaller uncertainties. The <<f(E1)>> systematic has been included to show the expected presence of the E1 transitions. The 6.5 MeV systematic prediction was decreased by the $E\gamma^2$ factor of the GDR E1 modelling, which decreases the accuracy, but can certainly be used as an indication.

The data shows a different trend compared to that in Fig. 3. It has a less distinct step form, with a lower part for nuclides with A < 150 and an increased one for heavier nuclides in reasonable agreement with the f(E1) systematics. The increased influence on the E1 strength for heavier nuclides is expected due to the decreasing energy of the E1 giant resonance. The sudden decrease of the PSF shape below A ~ 150 is difficult to explain. The OSLO data can be fitted both by polynomial and power law trend curves but the data dispersion below A < 150 remains large.

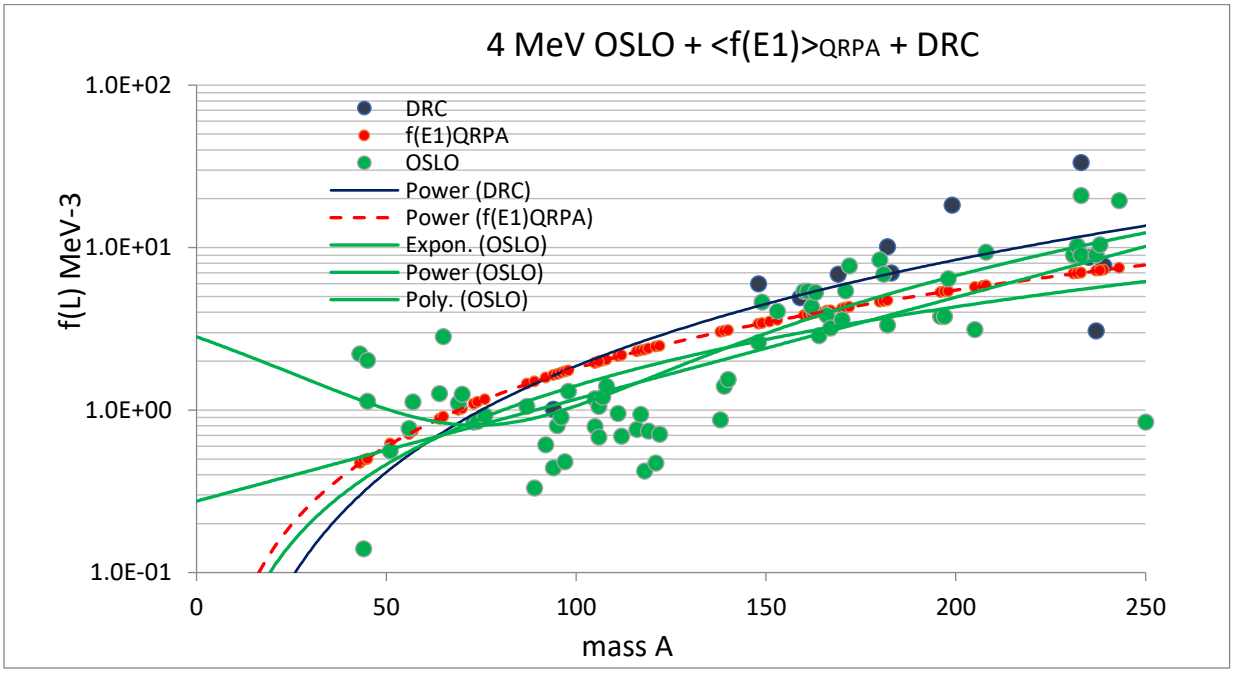

FIG. 4. The mid-energy 4 MeV OSLO PSF data points plotted as a function of the mass (all data has been averaged within the (4.0±0.5) MeV bin. Note again a sharp step of the PSF data at A ~ 150, which starts to increase again at A ~ 70. The agreement with the f(E1) systematics is rather good for heavier targets. The green curves are polynomial, exponential, and power functions fitted as eye guiding tools to show a wide uncertainty of the trend shape fitting.

It can be concluded that the data with masses above A ~ 150 reasonably follows the E1 GDR shape with the E1 mode dominating. This gives rise to the question as to what the reason for the data dip in the 90 < A < 140 range is.

The low energy region (<is2.0 MeV) – The low energy data is not supported by experimental evidence from other methods. The lowest energy data points lie between 1 -2 MeV with the average energy $\langle f(E_\gamma)\rangle$ = 1.4 MeV, their PSF values are plotted in Fig. 5 as a function of A. The absolute values are scattered around <f1(E1 + M1)> ~ 1.10^{-8} MeV^{-3} with no significant mass dependence which suggests that they are independent of the GDR tail. This conclusion is in contradiction with the GLO E1 model from Refs [5,6], the only model with a non-zero lim0

component. The constancy of the OSLO LEE is confirmed in Fig. 6 showing the internal fraction of the low energy <1.5 MeV> component against the medium <4 MeV> values. The relative decrease of the LEE component reflects the ratio of the constant LEE component against the increasing <4 MeV> values, with decreasing giant resonance energy.

The LEE, if it really exists, may play a significant role in the nucleosynthesis of nuclei with mass above A ~ 60 in a hot stellar environment through the r-process.

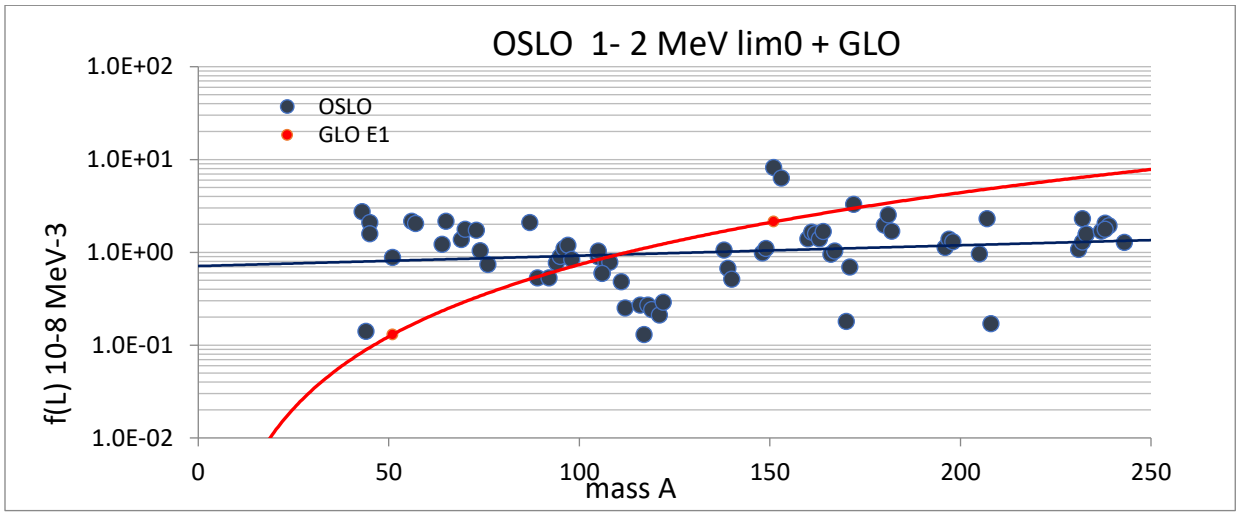

FIG. 5. The lowest OSLO PSF data points plotted as a function of the mass. An exponential trend curve gives a medium value of about 10^{-8} MeV^{-3}. The large dispersion of data may reflect the combination of experimental uncertainty and a postulated "upbend" limo component; no pronounced mass dependence has been detected. No effort for a trend shape projection to $E_\gamma \sim 0$ has been applied. The red curve gives the GLO calculation of the E1 radiation for gamma energy $E_\gamma \sim 0$.

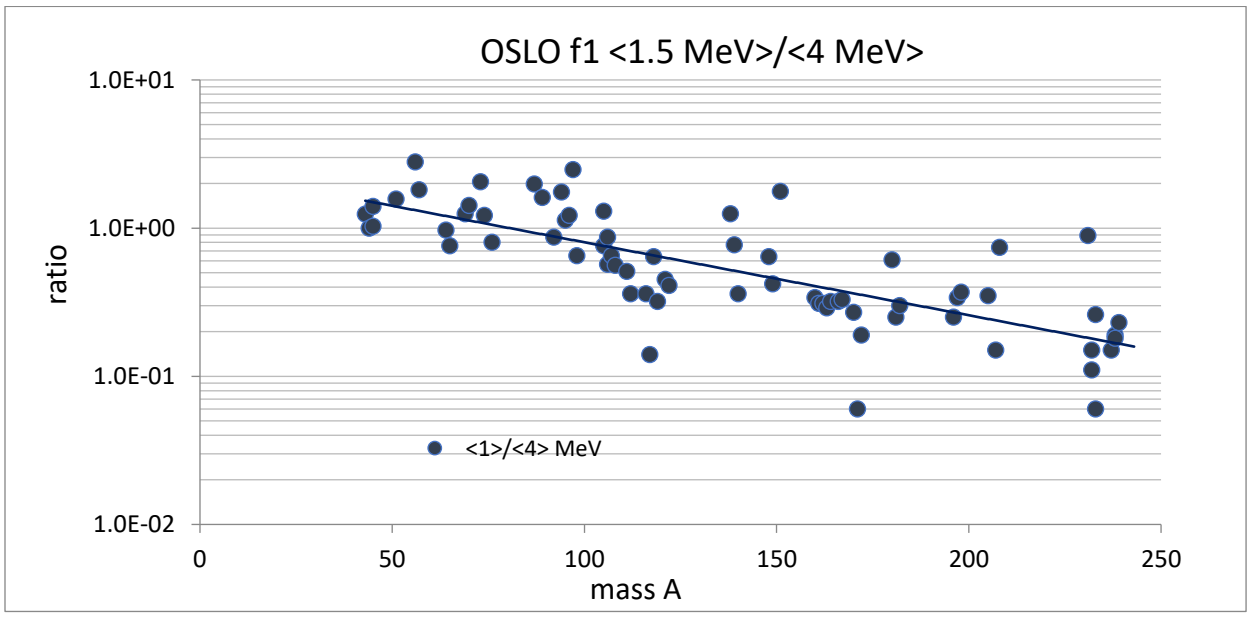

FIG.6. The ratio of the <1.5 MeV> against <4 MeV> data gives the internal relative dependence of these two PSF regions on the mass. Note the sharp decrease with A which may explain the "visual disappearance" of the LEE component for heavier nuclei compared to the increasing statistical E1 component (see more detail in the plot file).

3.2. Data uncertainties

The OSLO method has a complicated data analysis. The data uncertainties discussed in the 2019 CRP report [18] are considered below. The described experiment and calculational steps of the OSLO data analysis may give rise to several additional uncertainties. The statistical errors of the particle-γ coincidence data impact the solution of the matrix of initial excitation energy E_i bins versus the γ-ray energy Eγ. In the database readme file the quoted errors are given as: *Uncertainties from systematical error such as model dependent values have been accounted for*. However, several issues regarding the uncertainties need more attention because they influence the comparison of absolute PSF values:

1. There is a rather large difference in the given errors between data using the same data analysis and the reason is difficult to find. Two examples in Fig. 7 demonstrate the problem of the errors' inconsistency.

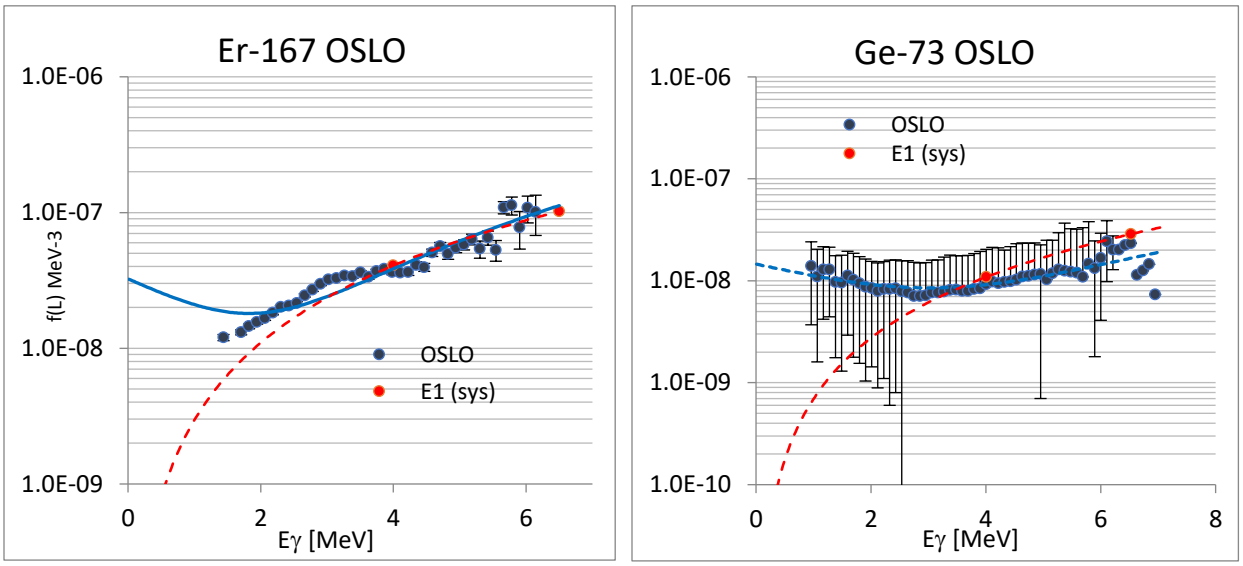

FIG. 7. Note the very small errors in the ^{167}Er data of the order of a few percent, which are typical of gamma-ray detection with a high-quality detection system. The errors in the ^{73}Ge data are huge and many of them have df1 > f1 (missing error bars). The blue curves are polynomial functions fitted to guide the eye. The red dashed curve is the f(E1) systematics.

2. Another uncertainty concern stems from the absolute normalization of the PSF, in which the transmission coefficients and the NLD parametrization are normalized (quote from the "readme" file text): *Absolute value of the level density and transmission coefficient is found by normalization to known values.* The choice of the NLD model used to extrapolate the discrete states and the D_0 spacing for the E_i and E_f energies influences the final PSF f1 curves, see Fig. 8 for the ^{140}La nucleus example, especially below 3 MeV.

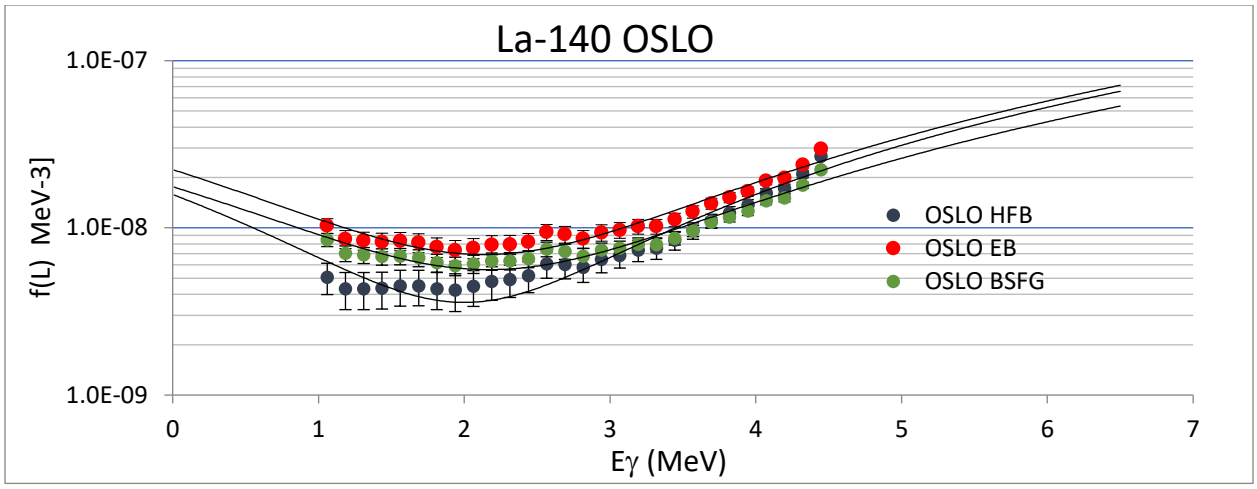

FIG. 8. The f1 data for the ^{140}La nuclide using three different NLD models in the normalization procedure. There is a difference of a factor of two between the final PSF data. The black curves are polynomial functions fitted to guide the eye.

3. In several OSLO entries the "upper, rec and low" limits are given for normalization. This procedure is not clearly explained, neither in the readme file nor in the original references. These normalization limits have a dramatic influence on the absolute f1 values shown in Fig. 9.

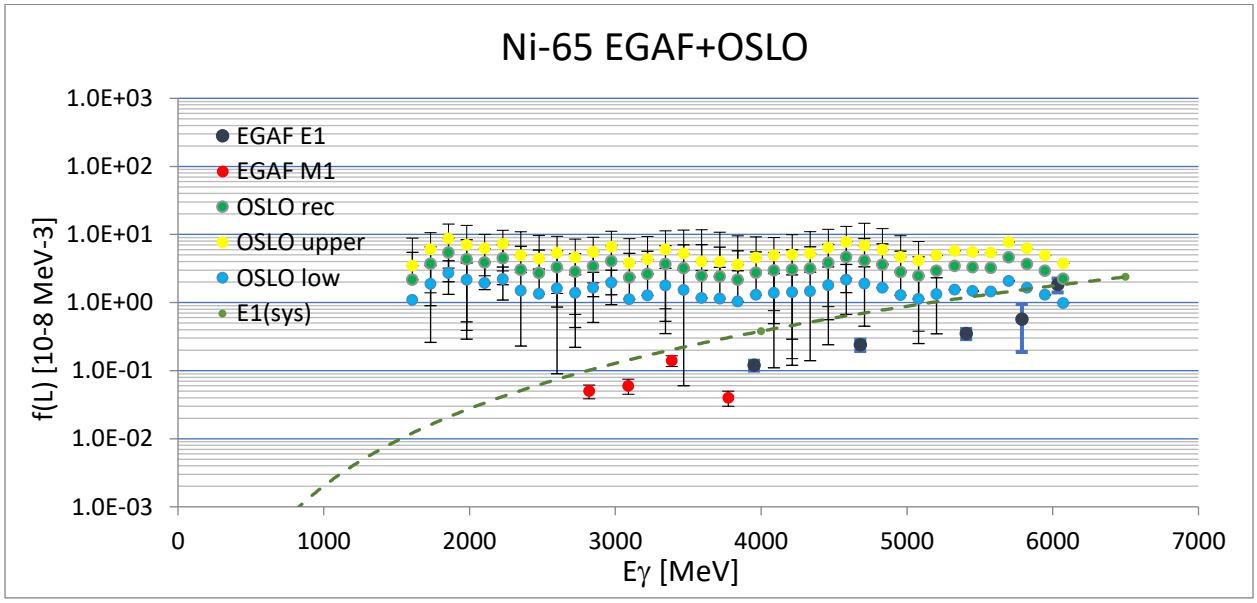

FIG. 9. Dispersion of f1 data of ^{65}Ni nucleus from 'upper, low and rec' normalizations, used for several data in the data base. The green dashed curve is the f(E1) systematics.

4. It is necessary to mention the processing error found and quoted in Ref. [19] which increases the absolute data uncertainties, prior to 2014, by an additional ~ 30% error. This correction suggests that there may be a systematic discontinuity in the absolute f1(E_γ) normalization between data before and after 2014, which should be accounted for.

5. Finally, the uncertainties from the unfolding procedure of the γ-ray spectra bins, by means of an iterative subtraction technique must be mentioned. Based on the experience we have with the DRC and ARC data processing (regarding the influence of empty bins on the averaging), it is worth questioning whether the energy bin with no gamma response in the OSLO experiment may influence the results. The answer can certainly be given by the OSLO specialists.

6. OSLO publications published after 2019 [Refs 20-25] introduce several methodological changes and improvements. Unfortunately, this data has not yet been included in the database and is therefore not discussed in this work. This data will certainly help to answer some of the above questions.

4. CONCLUSIONS

The OSLO data forms an impressive and robust wealth of photon strength functions in a broad energy region from 1.0 MeV up to the neutron separation energy S_n. The IAEA PSF 2019 database (CRP on Photonuclear Data and Photon Strength Functions (iaea.org)) edition includes 80 nuclides with OSLO data from ^{43}Sc up to ^{243}Pu. This the only method which is actively used to produce low energy PSF data for all masses. The main objective of the present study has been to address the OSLO data and summarize its performance compared to other PSF entries and/or the DRC systematics. For an overall visual inspection of this comparison, the plot file '*OSLO+PSF plot.docx'* is recommended. The obtained observations can be summarized, assuming a total uncertainty of 50% of the absolute normalization to account for the quoted and unquoted errors.

4.1. OSLO PSF shape and absolute normalization

1. The f1(E_γ) shape) is expected to be a smooth curve descending smoothly to lower E_γ values. The high energy (E_γ ~ < 4> and <6.5> MeV) OSLO data is in good agreement with the DRC systematics, but only for targets with A > 130 MeV. Data for lighter masses presents a sudden dip at this energy and underestimate the systematic prediction by a factor of three to six (see Figs 3 and 4).
2. Typical f1(E_γ) shapes for three target mass A regions as shown in Fig. 10 illustrate the main differences between the DRC systematic predictions. The chosen nuclides serve just as a demonstration. The decreasing role of the proposed LEE component, constant and independent of the nucleus mass (see Fig. 4), may be explained by the increasing GDR strength with mass A. This hypothesis, however, needs some modelling effort for confirmation. Any other idea, concerning the performance of the OSLO method at low E_γ and thus high E_i, would be an unjustified speculation.
3. The OSLO data strongly underestimates f (E1+M1) with respect to the <f(E1)> systematics (see ^{121}Sn shape results) whereas the D1M + QRPQ calculation supports the systematic curve (green curve in Fig. 10). This may suggest that the OSLO data decrease between 3

and 6 MeV is a problem. The inclusion of the missing M1 strength of the E1 systematics would make the disagreement even larger. The reason for this underestimation must be looked for (nuclear level densities?).

4. The light mass nuclides (for example the ^{45}Ti data) have a dominant LEE component below $E_\gamma \sim 4$ MeV, which is strongly above the f<E1>$_{sys}$ prediction. This component results from a convolution of the E1 and M1 radiation with an unknown ratio. There are no predictions to compare with, the DRC systematics below 3 MeV are not experimentally verified, and the theoretical modelling typically considers the E1 and M1 modes separately, due to differences in the collective excitations involved. This highlights a small disadvantage of the OSLO method since it measures combined E1 and M1 transitions.

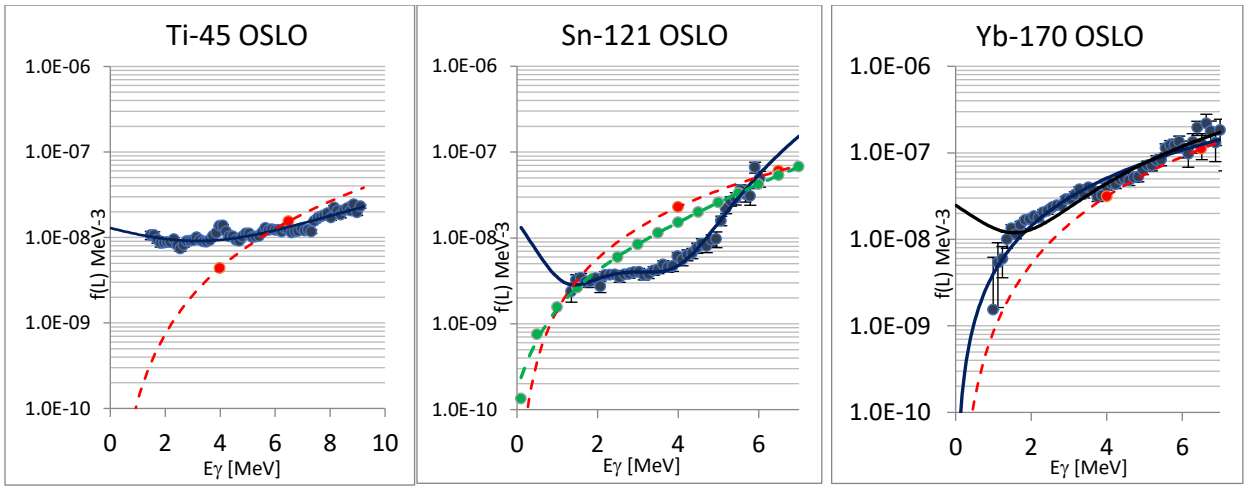

*FIG. 10. Three typical f1(E_γ) shapes as a function of the mas A. Note the extreme difference between the f1(E1+M1) shape and the <f(*E1>$_{syst}$ *trend (red dashed curve) below 4 MeV. Fits to OSLO data (blue curve) have an eye-guiding function only. The polynomial and power options are both plotted for the heavy A group to demonstrate the possible E1 and M1 strength uncertainty. The green dashed curve in the Sn-121 plot is the E1 D1M + QRPA calculation which agrees with the DRC systematics.*

4.2. OSLO uncertainties

The listing of uncertainties in Section 3.2. needs a confirmation by the original authors who implemented the method. The present crude assumption of a 50% uncertainty of the absolute f1(E_γ) values has been used only for a qualitative comparison with the DRC systematics. The impact of Porter-Thomas distribution on the added energy bins is neglected.

4.3. Future possibilities

The OSLO experiment is the only experimental source of PSF at low gamma ray energies and consequently high excitations close to the neutron binding energy. The data discussed in this work should be converted into a recommended (and well understood) database which may give significant information on the 'lim0' component behavior and could possibly be used for a trend analysis, like that from the neutron capture [8], and so accurately contribute to the lim0 estimates. The novel results from the recent work (see Refs [20-25]) should form the basis of such a work.

Acknowledgments

The authors appreciate the opportunity to collaborate, yet again, in the early twenties of the current century. They met in the early sixties of the last century in the Neutron Physics Department of the "UJV Rez" in Prague and remained colleagues and friends throughout their long professional careers in different countries.

JK gratefully acknowledges the financial support of the IAEA and thanks Stephane Goriely for his help and advice with the averaged D1M + QRPA data.

Technical remarks

The plotted OSLO data is fitted with the Excel trendline option, the curves have a purely eye guiding function. Where applicable, a polynomial trend function with the "expected" increasing upbend component below 1 MeV was included. For several nuclides the data points could not be fitted with a proper polynomial trend curve at all.

References

[1] G. Bartholomew et al., Adv. Nucl. Phys. **7** (1973) 229.
[2] R.G. Greenwood and R.E. Chrien, Nucl. Instr. Meth. **138** (1976) 125.
[3] P. Axel, Phys. Rev. **126** (1962) 671.
[4] S. Goriely and V. Plujko, Phys. Rev. C **99** (2018) 014303.
[5] S.G. Kadmenskij et al., Sov. J. Nucl. Phys. **37** (1983) 165.
[6] J. Kopecky and M. Uhl, Phys. Rev. C **41** (1990) 1941.
[7] J. Kopecky et al., Phys. Rev. C **47** (1993) 312.
[8] J. Kopecky, IAEA report INDC(NDS)-0799 (2020), https://www-nds.iaea.org/publications/indc/indc-nds-0799/
[9] J. Kopecky, IAEA report INDC(NDS)- 0815 (2020), https://www-nds.iaea.org/publications/indc/indc-nds-0815/
[10] J. Kopecky and S. Goriely, IAEA report INDC(NDS)-0821 (2020), https://www-nds.iaea.org/publications/indc/indc-nds-0821/
[11] J. Kopecky and S. Goriely, IAEA report INDC(NDS)-0839 (2022), https://www-nds.iaea.org/publications/indc/indc-nds-0839/
[12] A. Schiller et al., Nucl. Instr. Methods Phys. Res., Sect. A **447** (2000) 498.
[13] A. Voinov et al., Phys. Rev. Lett. **93** (2004) 142504.
[14] M. Guttormsen et al., Phys. Rev. C **71** (2005) 044307.
[15] M. Martini et al., Phys. Rev. C **94** (2016) 014304.
[16] J. Kopecky, private communication.
[17] S. Goriely et al., Phys. Rev. C **98** (2018) 014327.
[18] S. Goriely et al., Eur. Phys. J. A **55** (2019) 172.
[19] T. Renstrom T. et al., Phys.Rev. C **98** (2018) 054310.
[20] F. Zeiser et al., Phys.Rev. C **100** (2019) 024305.
[21] C.P. Brits et al., Phys. Rev. C **99** (2021) 054330.
[22] K.L. Maalatji et al., Phys. Rev. C **103** (2021) 014309.
[23) M. Wiedeking et al., Phys.Rev. C **104** (2021) 014311.
[24] M. Guttotmsen et al., Phys. Rev. Lett. **316** (2021) 136206.
[25] J. E. Mitbo et al., Comp. Phys. Comm. **262** (2021) 107795.

Nuclear Data Section
International Atomic Energy Agency
Vienna International Centre, P.O. Box 100
A-1400 Vienna, Austria

E-mail: nds.contact-point@iaea.org
Fax: (43-1) 26007
Telephone: (43-1) 2600 21725
Web: http://nds.iaea.org